HHS Public Access

Author manuscript

Organs Chip. Author manuscript; available in PMC 2023 March 01.

Published in final edited form as:

Organs Chip. 2022 December ; 4: . doi:10.1016/j.ooc.2022.100017.

Perfusable cell-laden micropatterned hydrogels for delivery of spatiotemporal vascular-like cues to tissues

Walter B. Varhue[a,1], **Aditya Rane**[b,1], **Ramon Castellanos-Sanchez**[c], **Shayn M. Peirce**[c], **George Christ**[c], **Nathan S. Swami**[a,b,*]

[a]Electrical and Computer Engineering, University of Virginia, Charlottesville, VA, 22904, USA

[b]Chemistry, University of Virginia, Charlottesville, VA, 22904, USA

[c]Biomedical Engineering, University of Virginia, Charlottesville, VA, 22904, USA

Abstract

The integration of vasculature at physiological scales within 3D cultures of cell-laden hydrogels for the delivery of spatiotemporal mass transport, chemical and mechanical cues, is a stepping-stone towards building *in vitro* tissue models that recapitulate *in vivo* cues. To address this challenge, we present a versatile method to micropattern adjoining hydrogel shells with a perfusable channel or lumen core, for enabling facile integration with fluidic control systems, on one hand, and to cell-laden biomaterial interfaces, on the other hand. This microfluidic imprint lithography methodology utilizes the high tolerance and reversible nature of the bond alignment process to lithographically position multiple layers of imprints within a microfluidic device for sequential filling and patterning of hydrogel lumen structures with single or multiple shells. Through fluidic interfacing of the structures, the ability to deliver physiologically relevant mechanical cues for recapitulating cyclical stretch on the hydrogel shell and shear stress on endothelial cells in the lumen are validated. We envision application of this platform for recapitulation of the bio-functionality and topology of micro-vasculatures, alongside the ability to deliver transport and mechanical cues, as needed for 3D culture to construct *in vitro* tissue models.

Keywords

Microfluidics; 3D cell culture; Biofabrication; Organ-on-a-Chip; *In vitro* vasculature models

*Corresponding author. University of Virginia, 351 McCormick Rd, Charlottesville, VA, 22904, USA. nswami@virginia.edu (N.S. Swami).

[1]Equal Contributors.

Author information

The manuscript was written through contributions of all authors and all authors approved the final version. The authors do not have financial interests related to the scientific results reported in the manuscript.

Declaration of interests

The authors declare that they have no known competing financial interests or personal relationships that could have appeared to influence the work reported in this paper.

Appendix A. Supplementary data

Supplementary data to this article can be found online at https://doi.org/10.1016/j.ooc.2022.100017.

1. Introduction

The development of *in vitro* tissue models that recapitulate the complex physiological environment and cues present within *in vivo* tissues is widely recognized as a core need for bioengineering applications, such as drug testing, regenerative medicine, tissue engineering, and disease modelling. Early approaches to reproduce these environments *in vitro* utilized two-dimensional (2D) cell culture models with engineered interfaces between the different cell types, such as an artificial membrane model (Yang et al., 1997), cone and plate model (Dewey et al., 1981) and the standard trans-well membrane system (Guo et al., 2008), (Garcia et al. 2004). While these approaches allow for transport of metabolites between the associated cell types, their chief failing is the suppression of signalling pathways associated with intercellular mechano-transduction due to the isolation of neighbouring cell types. Additionally, the cells are often placed against materials that are far stiffer than those encountered *in vivo*, thereby limiting the role of compliance and shear, as well as the signals delivered through extracellular matrix interactions.

Hydrogel-based 3D cell culture models (Ford et al., 2006) can recapitulate these native-like environmental and material cues. However, integration of 3D cell-laden hydrogel cultures with resistance vessels (≈100–200 μm) and microvasculature (arterioles of ≤100 μm and capillaries of ≈5–10 μm) at physiologically relevant scales has remained a challenge. Beyond facilitating nutrient delivery and waste removal, these vessel structures also shape mass transport in important ways, due to the intimate juxtaposition of the endothelial lining surrounding perivascular cell structure (such as vascular smooth muscle cells), and the adjacent tissues (Fig. 1A). The conformation of tissue interfaces around the vasculature, in relation to these spatiotemporal cues are significant for angiogenesis, immune response, cell migration, and metastasis. (Keenan and Folch 2007) Mechanical cues delivered to the surrounding vasculature profoundly influence cell architecture and function. Their recapitulation requires the ability to modulate flow conditions within a perfusable lumen. (Dai et al., 2004), (Polacheck et al., 2019). Across the circulatory system, there are wide variations in diameter of the vessels and the flow rate of blood through them, which affect the delivered shear stress to the endothelial wall (1–6 dyn/cm^2 for veins and 10–70 dyn/cm^2 for arteries) (Abaci et al., 2013). Perivascular cells, shielded by the endothelium, experience low rates of shear as a result of interstitial flow. (Wang and Tarbell 1995) Furthermore, the pulsatile fluid flow delivered to the relatively elastic arteries, veins and surrounding tissues can result in an increase in lumen diameter over short durations. The resulting cyclical stretch (Fig. 1B) of surrounding tissues influences the alignment of endothelial cells (ECs) (Fig. 1C) and perivascular cells, such as smooth muscle cells (SMCs) (Reinhart-King et al., 2008). Hence, perfusion systems are needed to recapitulate multiscale vascular anatomy, as well as to independently control flow rate, lumen pressures, and temporal flow profiles to a high degree of spatial resolution (Abaci et al., 2013). Current biofabrication methods are limited in their ability to recreate perfusable lumens of 3D hydrogel biomaterials, along with the associated multicellular topologies at physiological scales (Kim et al., 2017), (Xie et al., 2020). This limits the ability to recapitulate tissue-to-tissue interactions as found in natural tissues (Shen et al., 2008), as well as to deliver physiological scale flow rates and pressures to 3D cell-laden hydrogels. (Kim et al., 2017).

Microfluidic systems based on PDMS (poly-di-methyl siloxane) offer a diverse range of methods for precise flow and pressure control, as well as for recapitulating complex physiological flow states (Abaci et al., 2013), (Estrada et al., 2011), (Dong et al., 2019). This platform benefits from ease of integration with fluidic control systems, thereby allowing for a high level of spatial/temporal control of perfusion parameters. However, there are few reports on the integration of hydrogel lumens within microfluidic systems for delivering cues to 3D cultures. Most prior reports on microfluidic delivery of cyclical stretch or disturbed fluid flow cues are focused on conventional 2D cell cultures or require complex mechanical apparatus external to the lumen which only facilitate stretch in a single direction. (Abaci et al., 2013), (Shimizu et al., 2020)

We present a strategy for the fabrication of micropatterned single and multi-shell hydrogel structures (henceforth called microgels) that function as perfusable lumens that are aligned within a PDMS superstructure for enabling their facile integration with fluidic control systems. In this manner, spatially and temporally controlled fluidic cues can be delivered to cells and tissues during 3D culture. Our fabrication method combines microfluidic and imprint lithography methods to pattern these microgels with high-resolution lumens. Imprint lithography and micromolding have demonstrated the capability to replicate micron to submicron-scale grooves, channels, or textures within biomaterials. (Su et al., 2015), (Heidari and Taylor 2020) However, since hydrogel patterning occurs only over the imprinted surface, a large region of residual biomaterial is situated away from the patterned region. Conversely, microfluidic patterning offers a method to significantly restrict the bounds of the hydrogel structure, but it is often limited in its ability to pattern negative spaces internal to the gel structure, such as for adding grooves or channels (Caliari and Burdick, 2016). Our methodology of microfluidic imprint lithography (MIL) utilizes the high tolerance and reversible nature of the bond alignment process to lithographically position imprints within a microfluidic device to enable the sequential filling and patterning of lumens of microgels, thereby leveraging the benefits of both parent processes. PDMS microfluidic channels, which can be fabricated at high-resolution by micromolding from lithographically patterned SU8 resists are used to bound the outer dimension of the microgel lumen, while other PDMS imprint structures shape the inner dimension of the microgel lumen, thereby creating groove, channel, or internal patterns. Once aligned and reversibly bonded together, the outer microchannel and imprint structure form a sealed cavity that tightly confines the extent of any resulting hydrogel structure, thereby preventing any residual layer of hydrogel outside of the patterned area. This, in conjunction with high-resolution lithographic alignment, allows for each subsequently patterned structure to be aligned independent of the previously formed structure, thereby enabling the fabrication of nested, freestanding, and interfaced microgels. Following patterning, the resulting microgel structure can either be released from the microfluidic channel to create stand-alone structures or can remain inside the scaffolding provided by the PDMS superstructure, so that each lumen can be individually addressed by fluidic cues. The PDMS superstructure also acts to reinforce the microgel lumen structure to allow for perfusion to deliver chemical cues at physiologically relevant flow rates and pressures. Fluidic interfacing to the shell of the microgel lumen structures is validated by presenting the delivery of physiologically relevant mechanical cues for recapitulating shear stress and cyclical stretch factors to cells within the

structure. In this manner, not only do we create the necessary bio-functionality and topology of micro-vasculatures, but we also create the critical features of relevance to biological flow, such as the ability for pulsation, modifiable wall compliance, and induced wall shear stress, which can eventually create the cues needed to recapitulate micro-vasculature growth in patterned and perfusable 3D culture systems.

2. Results and discussion

2.1. Design of single-imprint lumen structures

To fabricate a perfusable micron-scale hydrogel structure (microgel) integrated within a PDMS superstructure, a combined microfluidic patterning and aligned imprinting process is utilized. This so-called microfluidic imprint lithography (MIL) method uses a PDMS ‘core imprint’ component to define the “open” areas forming the perfusable lumen of the microgel (Fig. 2A). This component is then aligned to the ‘shell microchannel’ using a bond alignment process (see Methods section & ESI S1†). To prevent contact between the PDMS chip and the bond chuck during alignment by wedge error correction (WEC), a metal frame is used to parallelize the two pieces over a fixed distance. The core imprint component is then inserted into a ‘shell’ microchannel, which defines the microgel’s outer diameter and acts as structural reinforcement for perfusion. The lumen imprint is reversibly bonded to the channel under external pressure to create an enclosed microchannel that defines the microgel dimensions. Hydrogel (composed of gelatin methacrylate or GELMA) is filled into the microchannel through a syringe pump and then cured using the UV crosslinking method to form the microgel. To improve adhesion of the gel within the microchannel, a methacrylate silane layer is deposited on the shell microchannel prior to alignment. The ‘core imprint’ is then de-bonded to define the lumen of the hydrogel lined microfluidic channel. To facilitate a clean release and prevent damage to the microgel pattern, the PDMS ‘core imprint’ is treated with an anti-stiction layer (1% BSA or Bovine Serum Albumin). After release the channel can be sealed to form a perfusable microgel embedded in a PDMS superstructure. Rigidity of the PDMS components can be tailored according to their function, by varying the base to curing agent ratio and the curing temperature, with high rigidity components used for the imprint structure and high compliance components used for application requiring cyclical stretch.

2.2. Patterning of single-imprint lumen structures

The versatility of the microfluidic imprint lithography method is presented by constructing patterned structures of single microgel lumens for potential application within 3D co-culture systems. The most basic architectures comprise of a single hydrogel biomaterial that needs only a single imprint step. Fig. 2B.i presents an example structure designed for possible coculture application with endothelial cells (ECs) that is comprised of a straight perfusable lumen, surrounded by a physiologically relevant hydrogel shell, which would have ECs cultured on the inside surface of the lumen, while the hydrogel would be laden with perivascular cells or other cells of interest (expanded process flow in ESI S1 Fig. S1a†). The thickness of the hydrogel shell is designed based on the typical mass transport distances *in vivo*, of 100–200 μm away from the vessel. This perfusable microgel is reinforced by a PDMS superstructure, with a rigidity tuned to allow for appropriate cyclical stretch under

pulsed physiological scale fluid flow. For this design (Fig. 2B.i), the dimensions of a rat carotid artery were used as a model. To replicate this pattern, a 1 cm long straight lumen imprint with a height of 250 μm and a width of 480 μm is aligned within a 1.5 cm long and 375 μm high by 750 μm wide straight channel. This resulted in a hydrogel shell (130 μm thickness) around a 1 cm long perfusable lumen, with dimensions identical to the insert. Once formed, this device can be aligned and bonded with an identical device to create an enclosed 500 μm by 500 μm square lumen. It can also be bonded to a glass cover slip forming a half lumen, for enabling facile imaging using inverted microscopy. While perfusable lumens used for culture of ECs of similar dimensions have been demonstrated previously (Zheng et al., 2012; Song et al., 2018; Mannino et al., 2017; Chrobak et al., 2006; Zhang and Larsen, 2017) these lumens are typically surrounded by a far more extensive hydrogel structure, which limits adequate mass transport from the lumen into the biomaterial, thereby causing significant loss of viability of cultured cells. In the reported method, on the other hand, the thickness of the biomaterial shell around the perfusable lumen is significantly limited to ensure that the transport of chemical cues across the cultured EC layer resemble *in vivo* length scales. Another single imprint architecture (Fig. 2 B.ii & 2D.i-ii) is a microgel containing two individually addressable perfusion channels, with an interceding hydrogel structure (500 μm wide), as would be used for creating chemotactic gradients for cells laden in the hydrogel (Baker et al., 2013) (expanded process flow in ESI S1 Fig. S1b†). For this structure, 500 μm high by 500 μm wide lumens were formed simultaneously within a microgel that is integrated in a PDMS channel (2 mm wide by 500 μm high). These parallel channels maintain their 500 μm separation over a length of 1 cm. The two lumens are fluidically addressable, since the two lumens branch away from each other through individual channels outside of this overlap region to independent sets of inlets and outlets. This ability to address each channel is demonstrated in Fig. 2D.ii, wherein one channel is filled with PBS (phosphate buffered saline) containing 1 mg/mL FITC labelled Poly--L-lysine and the adjoining channel with the respective unlabelled fluid. Devices with similar architecture have been demonstrated for studies of chemoattractant gradients, endothelial cell sprouting, organ-on-chip studies, and cell co-culture. (Baker et al., 2013; Lin et al., 2019; Zhu et al., 2020) However, in these cases the liquid gel interface can be maintained only over a limited length (10–100 μm scale), with support structures required to maintain surface tension during hydrogel patterning or the need for embedded sacrificial 3D printed features that create unused surrounding hydrogel structures. In the MIL method, on the other hand, since the patterned imprint component is responsible for defining the configuration of the liquid gel interface, the width of the perfusable channels and the width of the gel separating the adjoining channels can be tailored over a much greater spatial extent of active region. For instance, the lumen width can be varied to create a gradation in shear stress along the channel length or the hydrogel width can be modulated to alter the diffusional profile of species through the hydrogel. Finally, since vasculatures consist of circular lumens, we use a curved master for the core imprint that is subsequently molded in PDMS to analogously create circular hydrogel structures of different cross-sectional regions (Fig. 3A–B). To create curved structure lumens that are enclosed by the hydrogel on all sides (i.e., no PDMS in lumen), we reversibly bond two PDMS superstructures containing the hydrogel patterns (Fig. 3C. i) to create the hydrogel enclosed lumen (Fig. 3C. ii). Rectangular lumen cross-sections enable well-defined edges that permit facile lithographic

alignment of multilayer structures, while this is harder to accomplish with circular structures that have regions out of the focal plane. To make the alignment process easier, matching alignment marks were used for the shell and the core to permit alignment on a standard mask aligner, prior to filling of the hydrogel and its curing to create circular lumens.

2.3. Design of multiple-imprint biomaterial structures

To integrate multiple types of patterned biomaterial structures within the perfusable microgel, this process needs to be repeated with a second imprint component. However, to avoid desiccation of the hydrogel, the time-consuming interlayer alignment steps are performed on the mask aligner prior to introduction of the hydrogel material. Hence, after the first hydrogel pattern is formed, a method to rapidly re-align the previously aligned core and shell components is developed to pattern subsequent hydrogel structures, per Fig. 4A. For this purpose, the second imprint component is first aligned to the microchannel by the previously outlined methods. After the reversible bonding step, re-alignment guide holes are drilled through two aligned components in a configuration set by a 3D printed holder, using a biopsy punch. The aligned components are then mounted on a 3D printed scaffold using pins that correspond to the layout of drilled alignment holes. The channel is then released, leaving the imprint core still mounted on the scaffold. The first microgel patterning step is then completed as outlined above. After the first microgel has been formed, the channel is then rapidly re-aligned to the second imprint core by mounting it back on the scaffold using the pins and alignment holes. A second biomaterial can then be filled into the device and crosslinked to form a multi-material microgel structure.

2.4. Patterning of multi-biomaterial lumen structures

To highlight this ability to rapidly re-align subsequent imprint cores after an initial hydrogel patterning step, we present the formation of perfusable microgels featuring multiple types of individually patterned biomaterial structures (Fig. 4B. i-ii). These can be utilized towards the creation of engineered liquid tissue biomaterials and tissue-tissue interfaces of relevance to co-culture systems (Li et al., 2012) (Kunze et al. 2011). To create lumens with nested hydrogels of multiple biomaterials (Fig. 4C. i-ii), a second lumen imprint with smaller dimensions is aligned within the lumen formed during the initial patterning step (expanded process flow in ESI S1 Fig. S1c†). After alignment, a second hydrogel can be introduced to form the inner shell. The resulting perfusable hydrogel structure features a single 500 μm wide by 300 μm high lumen, surrounded on three sides by two nested hydrogel layers of 125 μm thickness.

For application to co-culture systems, each of these hydrogel layers would be laden with a different set of target cells. While similar nested gel interfaces have been demonstrated in other work (Hasan et al., 2015), in these cases the outer diameter of the gel layer is not defined, which can limit perfusion due to significant differences in scale between the two tissue structures. On the other hand, the structures we present here seek to replicate the size scale over which mass transport would occur from vessels to the surrounding tissue *in vivo*, thereby allowing for tissue-to-tissue interactions that lead to the formation and preservation of chemical gradients across tissues or for variations in nutrient, dissolved oxygen, or other chemical cue levels.

2.5. Design of multi-hydrogel interface structures

Through multiple imprint steps, it is possible to utilize the MIL process for the fabrication of more complex 3D interfaces between perfusable biofunctional hydrogel structures, such as those of different hydrogel materials or those laden with different cell types. While open space within the microgel formed during the imprint step has been used in the prior section as a perfusable lumen, we utilize it here to pattern gel-to-gel interfaces by filling-in the open space with another hydrogel. In these applications, the first imprint is used to define the lumen and the hydrogel barrier, which then functions as one side of the gel-to-gel interface. Such imprints are designed with a feature, which after appropriate alignment, can limit hydrogel flow to a portion of the shell microchannel, thereby patterning the spatial extent of the resulting structure. A second hydrogel precursor may then be filled into the portion of the microchannel and crosslinked. During this step a second imprint may be aligned by the process outlined above within this open space, forming a perfusable channel within the second hydrogel structure, as well as the gel-to-gel interface (Fig. 5A).

2.6. Patterning of multi-hydrogel interface structures

To highlight this feature, we present a 2 mm wide composite structure comprised of two individually patterned hydrogel biomaterials, with an engineered interface between them. This structure is positioned between two parallel individually addressable perfusable 500 μm wide microchannels (Fig. 5B), similar to the single material iteration described above (expanded process flow in ESI S1 Fig. S1c†). The overall combined width of the hydrogel structure remains consistent over the 7.5 mm length that the parallel channels interact over. To demonstrate the versatility possible by this design, Fig. 5C.i-iii shows that the position of the interface between the two gels can be varied, as may be required for a 3D co-culture system that allows for monitoring of the interactions between two types of cells embedded in the respective hydrogels. Additionally, since perfusable channels are formed, nutrients can be delivered to the cells in each hydrogel. This also allows for the formation of gradients of analytes and drugs to be tested. Other methods to obtain gel to gel interfaces within microfluidic channels have been reported (Shin et al., 2012), (Kunze et al. 2011), (Lee et al., 2020), but these methods rely on surface tension or hydrodynamic forces to pattern the interface. Hence, they can only maintain this interface over a limited length (10–100 μm scale), while not allowing for a high degree of variation in the architecture of the patterned gel-to-gel or gel-to-liquid interface, or their feature sizes are at a millimeter size scale. In the reported case, on the other hand, since the dimensions of both, the lumen and the interface are defined by the micropatterned insert, a far wider variation in architecture is possible.

2.7. Validation of cyclic stretch and shear stress cues in perfusable microgels

Mechanical factors associated with pressure driven blood flow, such as wall shear stress and cyclic stretch, vary widely throughout the cardiovascular system and have profound influence on the cellular architecture and function of the tissues surrounding blood vessels (Abaci et al., 2013). Differences in vessel lumen diameter, blood flow rates, and degree of exposure to blood flow influence the delivered shear stress to the surrounding cells. For endothelial cells (ECs), which are directly exposed to blood flow, shear stress ranges from 1 to 6 dyn/cm^2 for veins and 10–70 dyn/cm^2 for arteries. (Abaci et al., 2013).

On the other hand, smooth muscle cells (SMCs) within healthy vasculature experience limited shear stress levels due to interstitial flow (1–3 dyn/cm^2). However, in circumstances of endothelium disruption, SMCs can experience higher shear stress (10–20 dyn/cm^2). Furthermore, the pulsatile blood flow profile driven by the heart to large diameter vessels, such as arteries and veins, causes fluctuations in lumen diameter that results in cyclical stretch of surrounding tissues. Shear stress and cyclic stretch act in tandem to align endothelial and perivascular cell configurations (Wang and Tarbell 1995). Given the wide range of physiological effects caused by shear stress and cyclic stretch to vasculature cells (SMCs and ECs), there is a need to tailor the flow states for maintaining an adequate perfusion level and facilitating mass transport, so that the *in vitro* model replicates the relevant homeostasis or disease state under investigation. However, fluidic control for recapitulation of the cues within perfusable hydrogel-based 3D culture environments is yet to be demonstrated. Herein, we validate ability of the patterned and perfusable microgels that are supported within the PDMS superstructure to withstand the required pressures and flow rates, by using external tuning elements (hydrodynamic resistors, pressure and flow rate sensors) for delivering biomimetic mechanical factors (Fig. 6A).

Shear stress in microfluidic culture is usually modulated by the flow rate and dimensions of the device, while cyclical stretch is determined by the gauge pressure and the Young's modulus of the materials in the device. Facile control of shear stress in the channel can be achieved by altering flow rates, but a similar method to independently control cyclic stretch through delivered fluid flow is not possible. Typically, cyclic stretch is controlled by varying external air pressure and internal fluid pressure over a flexible membrane or by stretching the channel using a specialized external mechanical stage (Estrada et al., 2011), (Shimizu et al., 2020), but this limits the stretch to a single direction and it is often localized over only a limited region of the channel. In the current work, on the other hand, we alter the level of cyclic stretch independent of the flow rate, by utilizing a PDMS superstructure of high compliance (curing agent ratio of 1–20) to set the Young's modulus of the device material, while tuning input and output resistors from the microgel to vary the peak value of a pulsed pressure source, resulting in an increase in lumen diameter (Fig. 6B.ii). Per device schematic in Fig. 6A and the equivalent fluidic circuit in Fig. 6B.i, the input pulmonary (R_P) and output aortic resistors (R_A) to the perfusable hydrogel channel device are set based on tubing length, so that this net system resistance ($R_{sys} \approx R_P + R_A$) can be used to fix flow rate and the resulting shear stress (Oh et al., 2012). Analogously, the ratio of the length of the aortic element to the combined length of aortic and pulmonary elements is used to vary the pressure correction (PC) factor to alter the pressure pulse for creating cyclic stretch. In this manner, the effects of cyclical stretch on the hydrogel lumen can be explored in tandem with shear stress-induced cues for alignment of endothelial cell morphology along the flow direction in the perfusable hydrogel channel. Per the detailed equations in ESI S2†, by carefully choosing R_P and R_A, the values of PC and R_{sys} can be set independent of each other for precise tuning of the flow rate and pressure within the lumen (Fig. 6C.i-ii), thereby ensuring a relatively uniform gauge pressure and cyclical stretch along the length of the perfusable channel. Based on the dimensions of the lumen, viscosity of the perfused media, and the range of delivered flow rates, several ranges of shear stress may be delivered within the above device for various SMC and EC models (Fig. 6C. ii), including arterial and venous

ECs, as well as for normal SMCs and those with disrupted ECs. Table 1 presents the tuned resistance values (R_{sys}, R_A, and R_P) required for a 500 mbar pressure pulse to deliver pulsed physiological flow rates consistent with these culture models (Abaci et al., 2013), (Abaci et al., 2013).

To demonstrate flow tuning, we utilize a 1 cm long, 250 μm high, and 480 μm wide perfusable hydrogel lumen structure comprised of a 10% gelatin hydrogel (enzymatically crosslinked by microbial transglutaminase or mTG), which is embedded in a 375 μm high by 750 μm wide microgel structure. An inline pressure sensor is utilized to optimize tuning resistors (R_P & R_A) that determine PC values of 0.8 and 0.4 to result in pressure pulses of 400 mbar and 240 mbar, respectively (Fig. 7A.i – 7A.ii). The resulting increase in lumen diameter due to cyclic stretch from initial state (t_1 = 2 s) to final state (t_2 = 3 s), under gauge pressures of 240 mbar and 400 mbar, is measured by microscopy (computations in ESI S3†) as: 5.9% and 11%, respectively (Fig. 7B.i – 7B. ii). This is in line with physiological expectations, wherein cyclical stretch levels range between 5% and 10%, respectively. (Estrada et al., 2011). For visualization, these two states of low and high shear stress are shown using beads in the perfusable hydrogel channel (Fig. 7C.i and 7C. ii) and the effect of the shear stress cues on endothelial cell morphology in the channel is shown in Fig. 7D.i (static culture) versus Fig. 7D.ii (dynamic culture at 600 μL/min). Hence, through embedding the perfusable microgel in a compliant PDMS superstructure with a curing ratio that is adjusted to resemble the stiffness of typical tissues (~0.84 MPa), the microgel channel can undergo cyclic stretch (expand and return to its original state) at biomimetic levels upon being pressurized under fluid flow and can exhibit shear stress under the same flow rate cues.

3. Methods

3.1. Lithographic alignment

The alignment and reversible bonding of the lumen imprint and the shell microchannel was achieved by a modified large gap alignment process, using a standard mask aligner (EV Group 620). The PDMS microchannel component was first mounted onto a 4-inch square soda lime glass plate, which was then loaded into the aligner such that it is face down towards the chuck, where the PDMS insert core component would be loaded. To ensure uniform separation during alignment and contact during temporary bonding, prior to loading the imprint core, a wedge error correction (WEC) process was run to parallelize the chuck, on which the core component would be loaded with the glass plate and on which the channel component was already mounted. To prevent damage to the channel component during this process, a frame was loaded in between the glass plate and chuck to allow the WEC pressure to be applied between the glass plate and the chuck, without requiring the loaded core component to come into contact with the chuck. After the WEC step, the imprint core was loaded onto the chuck and aligned to the channel using alignment marks. Due to the topography of the imprint core, a separation gap of 1 mm was needed during the alignment step. The software of the large gap alignment setting allowed for alignment of features that are not in the same focal plane. After the initial alignment step was finished, the channel was gradually lowered onto the insert, with fine corrections to alignment being made as the two

components are brought into close proximity with one another. Once assembled, pressure was applied to form a reversible bond between the two PDMS components, which were then unloaded from the mask aligner.

3.2. Channel fabrication

The outer PDMS channel and lumen imprint were replicated from either a SU-8 mold or 3D printed masters constructed using a standard soft lithography process. Negative master molds of both components were prepared using either SU-8 photolithography or 3D printing. In the case of the SU-8 on silicon masters, an anti-stiction silane layer was vapor deposited to improve mold release. Rigidity of the PDMS components was tailored by their base to curing agent ratio and curing temperature according to their function. For the imprint components, where higher rigidity was required to ensure pattern fidelity, a 10 to 3 base to curing agent ratio was used and the molds were cured on a covered hotplate for 3 h at 120 °C. The lumen imprint components were then treated with a 1% BSA solution for 15 min at room temperature, before blow drying with a high-pressure dry nitrogen source. Microchannels used in applications not designed for replicating cyclical stretch were produced by the same protocol, with the exception of the anti-stiction layer. Instead, if GELMA was being used for the microgel structure, a methacrylated silane adhesion layer was deposited on the channel device. In cases where cyclic stretch was being recapitulated, a lower rigidity was required to allow the microgels to deform under the high lumen pressures. Hence, a 20 to 1 base to curing agent ratio for PDMS was used and cured at room temperature for 24 h.

3.3. Fluidic perfusion and mechanical measurements

For applications that do not investigate cyclical stretch, the PDMS superstructure with the microgels were sealed by using a 3D printed scaffold to sandwich the device between two glass plates. The PDMS chip forms a reversible physical bond with the glass plate sealing the channel, while the 3D printed scaffold applies sufficient pressure to ensure that the bond withstands the lumen pressure during perfusion. To deliver fluid, flow inlet/outlets were drilled though one of the glass plates to allow for tubing to be inserted within the PDMS device (Varhue et al., 2017). For cases wherein higher compliance PDMS was required to facilitate cyclical stretch of microchannels during pulsed perfusion, an adhesive bonding method was used to bond a glass slide to the PDMS chip. After bonding, biomimetic temporal and mechanical factors were introduced by perfusing the channel with a peristaltic pump.

3.4. Endothelial cell culture in perfusable microgel

To study the effects of the perfusable microgel on endothelial cell (EC) viability and morphology, dermal EC’s were seeded and cultured under fluid flow for 24 h. Dermal endothelial cells (Cell Biologics) were expanded (4p-7p) in T-25 plates coated with gelatin 2%. Cell expansion was done using endothelial cell medium (Cell Biologics cat# C57-6064). Once confluency was reached, cells were plated out using TrypLE 10x (Fisher Scientific) and were then seeded within a microgel channel at a cell density of 10^5 cells per mL. The perfusable microgel channel prepared using the methods outlined in Fig. 2 featured a 1 cm long 375 μm high and 750 μm wide microgel structure aligned within a PDMS

superstructure with a 250 μm high and 480 μm wide perfusable lumen. The structure was comprised of a 10% gelatin (enzymatically crosslinked by microbial transglutaminase or mTG). Post seeding, the cells were left in static conditions for 4 h within the microgel channel to allow them to attach to the gel surface, after which a 600 μl/min fluid flow was delivered to the system using a peristaltic pump. A no-flow static condition device was also prepared where the cells were seeded in an open channel submerged within 5 mL of media. After 24 h cell morphology was imaged using an EVOS FL (life technologies) for both devices. The shear stress incident on the cells cultured within the device can be estimated at 17.8 dyn/cm^2, which is at the lower end of the reported physiological range (15–150 dyn/cm^2).

4. Conclusions

We present the application of microfluidic imprint lithography (MIL), as a novel method to fabricate high resolution perfusable microgel channels that can be integrated within a PDMS superstructure to deliver biomimetic spatio-temporal fluidic cues to cells and tissues in 3D culture systems. Specifically, we have demonstrated a range of possible microgel structures, including those that maintain the spatial component of mass transport from vasculature, strategies to pattern interfaces of multiple biomaterials, and highly versatile liquid-to-gel and gel-to-gel interfaces. Since these perfusable microgels are integrated within microfluidic channels, important mechanical factors, such as shear stress and cyclical stretch can also be delivered. Herein, we have shown that by embedding the perfusable microgels in a compliant PDMS superstructure, the microgel channel can exhibit biomimetic levels of cyclic stretch upon being pressurized under fluid flow cues and can exhibit shear stress under flow rate cues. We envision that this feature can eventually be utilized in future work towards orthogonal alignment of endothelial to smooth muscle cells, akin to their arrangement within micro-vasculatures. Prior methods for recapitulating these factors *in vitro* are typically limited to the delivery of only paracrine signalling (Lee et al., 2020), (Day et al., 2020) or just factors for shear stress using cone plates. These methods are further limited in their integration with 3D coculture systems and with biomaterials, such as cell laden hydrogels. Several microfluidic methods allowing the simultaneous delivery of shear stress and cyclical stretch with high degrees of accuracy have been demonstrated, but they rely on 2D culture of cells on PDMS or in other inorganic channel substrates, or on complex external mechanical stages which can only deliver stretch in a single direction. Although this current work only demonstrated the replication of flow cues at the top end of the physiological range, the integrated gel-PDMS devices would be compatible with other microfluidic methods for delivery of lower scale fluidic flow rates and pressures.

Supplementary Material

Refer to Web version on PubMed Central for supplementary material.

Acknowledgments

This work was supported from the AFOSR grant FA2386-21-1-4070 and from University of Virginia’s Strategic Investment Fund to establish the Center for Advanced Biomanufacturing (CAD-bio), Engineering in Medicine initiative and the School of Engineering’s Research Innovation Award.

References

Abaci HE, Devendra R, Soman R, Drazer G, Gerecht S, Apr. 2012. Microbioreactors to manipulate oxygen tension and shear stress in the microenvironment of vascular stem and progenitor cells. Biotechnol. Appl. Biochem. 59 (2), 97–105. 10.1002/bab.1010. [PubMed: 23586790]

Abaci HE, Drazer G, Gerecht S, Feb. 2013. Recapitulating the vascular microenvironment in microfluidic platforms, 03 Nano LIFE 1340001. 10.1142/S1793984413400011, 01.

Baker BM, Trappmann B, Stapleton SC, Toro E, Chen CS, Aug. 2013. Microfluidics embedded within extracellular matrix to define vascular architectures and pattern diffusive gradients. Lab Chip 13 (16), 3246–3252. 10.1039/c3lc50493j. [PubMed: 23787488]

Caliari SR, Burdick JA, Apr. 2016. A practical guide to hydrogels for cell culture. Nat. Methods 13 (5), 405–414. 10.1038/nmeth.3839. [PubMed: 27123816]

Chrobak KM, Potter DR, Tien J, May 2006. Formation of perfused, functional microvascular tubes in vitro. Microvasc. Res. 71 (3), 185–196. 10.1016/j.mvr.2006.02.005. [PubMed: 16600313]

Dai G, et al. , Oct. 2004. Distinct endothelial phenotypes evoked by arterial waveforms derived from atherosclerosis-susceptible and -resistant regions of human vasculature. Proc. Natl. Acad. Sci. Unit. States Am. 101 (41), 14871–14876. 10.1073/pnas.0406073101.

Day JH, et al. , 2020. Injection molded open microfluidic well plate inserts for user-friendly coculture and microscopy. Lab Chip 20 (1), 107–119. 10.1039/C9LC00706G. [PubMed: 31712791]

Dewey CF, Bussolari SR, Gimbrone MA, Davies PF, Aug. 1981. The dynamic response of vascular endothelial cells to fluid shear stress. J. Biomech. Eng. 103 (3), 177–185. 10.1115/1.3138276. [PubMed: 7278196]

Dong R, Liu Y, Mou L, Deng J, Jiang X, 2019. Microfluidics-based biomaterials and biodevices. Adv. Mater. 31 (45), 1805033. 10.1002/adma.201805033.

Estrada R, et al. , Apr. 2011. Endothelial cell culture model for replication of physiological profiles of pressure, flow, stretch, and shear stress in vitro. Anal. Chem. 83 (8), 3170–3177. 10.1021/ac2002998. [PubMed: 21413699]

Ford MC, et al. , Feb. 2006. A macroporous hydrogel for the coculture of neural progenitor and endothelial cells to form functional vascular networks in vivo. Proc. Natl. Acad. Sci. Unit. States Am. 103 (8), 2512–2517. 10.1073/pnas.0506020102.

Garcia CM, Darland DC, Massingham LJ, D'Amore PA, Aug. 2004. Endothelial cell-astrocyte interactions and TGF beta are required for induction of blood-neural barrier properties. Brain Res. Dev. Brain Res. 152 (1), 25–38. 10.1016/j.devbrainres.2004.05.008. [PubMed: 15283992]

Guo S, et al. , May 2008. Neuroprotection via matrix-trophic coupling between cerebral endothelial cells and neurons. Proc. Natl. Acad. Sci. Unit. States Am. 105 (21), 7582–7587. 10.1073/pnas.0801105105.

Hasan A, Paul A, Memic A, Khademhosseini A, Oct. 2015. A multilayered microfluidic blood vessel-like structure. Biomed. Microdevices 17 (5), 88. 10.1007/s10544-015-9993-2. [PubMed: 26256481]

Heidari H, Taylor H, Mar. 2020. Multilayered microcasting of agarose–collagen composites for neurovascular modeling. Bioprinting 17, e00069. 10.1016/j.bprint.2019.e00069.

Keenan TM, Folch A, Dec. 2007. Biomolecular gradients in cell culture systems. Lab Chip 8 (1), 34–57. 10.1039/B711887B. [PubMed: 18094760]

Kim S, Kim W, Lim S, Jeon JS, Jan. 2017. Vasculature-on-A-chip for in vitro disease models. Bioeng. Basel Switz. 4 (1) 10.3390/bioengineering4010008.

Kunze A, Valero A, Zosso D, Renaud P, Oct. 2011. Synergistic NGF/B27 gradients position synapses heterogeneously in 3D micropatterned neural cultures. PLoS One 6 (10). 10.1371/journal.pone.0026187.

Lee UN, et al. , 2020. Layer-by-layer fabrication of 3D hydrogel structures using open microfluidics. Lab Chip 20 (3), 525–536. 10.1039/C9LC00621D. [PubMed: 31915779]

Li X. James, Valadez AV, Zuo P, Nie Z, Jun. 2012. Microfluidic 3D cell culture: potential application for tissue-based bioassays. Bioanalysis 4 (12), 1509–1525. 10.4155/bio.12.133. [PubMed: 22793034]

Lin NYC, et al. , Mar. 2019. Renal reabsorption in 3D vascularized proximal tubule models. Proc. Natl. Acad. Sci. Unit. States Am. 116 (12), 5399–5404. 10.1073/pnas.1815208116.

Mannino RG, et al. , Jan. 2017. 3D microvascular model recapitulates the diffuse large B-cell lymphoma tumor microenvironment in vitro. Lab Chip 17 (3), 407–414. 10.1039/c6lc01204c. [PubMed: 28054086]

Oh KW, Lee K, Ahn B, Furlani EP, Feb. 2012. Design of pressure-driven microfluidic networks using electric circuit analogy. Lab Chip 12 (3), 515–545. 10.1039/c2lc20799k. [PubMed: 22179505]

Polacheck WJ, Kutys ML, Tefft JB, Chen CS, May 2019. Microfabricated blood vessels for modeling the vascular transport barrier. Nat. Protoc. 14 (5), 1425–1454. 10.1038/s41596-019-0144-8. [PubMed: 30953042]

Reinhart-King CA, Fujiwara K, Berk BC, 2008. Physiologic stress-mediated signaling in the endothelium. Methods Enzymol. 443, 25–44. 10.1016/S0076-6879(08)02002-8. [PubMed: 18772009]

Shen CJ, Fu J, Chen CS, Mar. 2008. Patterning cell and tissue function. Cell. Mol. Bioeng. 1 (1), 15–23. 10.1007/s12195-008-0005-y.

Shimizu A, Goh WH, Itai S, Hashimoto M, Miura S, Onoe H, 2020. ECM-based microchannel for culturing *in vitro* vascular tissues with simultaneous perfusion and stretch. Lab Chip 20 (11), 1917–1927. 10.1039/D0LC00254B. [PubMed: 32307467]

Shin Y, et al. , Jun. 2012. Microfluidic assay for simultaneous culture of multiple cell types on surfaces or within hydrogels. Nat. Protoc. 7 (7), 1247–1259. 10.1038/nprot.2012.051. [PubMed: 22678430]

Song KH, Highley CB, Rouff A, Burdick JA, 2018. Complex 3D-printed microchannels within cell-degradable hydrogels. Adv. Funct. Mater. 28 (31), 1801331. 10.1002/adfm.201801331.

Su Y-H, Chiang P-C, Cheng L-J, Lee C-H, Swami NS, Chou C-F, Dec. 2015. High aspect ratio nanoimprinted grooves of poly(lactic-co-glycolic acid) control the length and direction of retraction fibers during fibroblast cell division. Biointerphases 10 (4). 10.1116/1.4936589, 041008.

Varhue WB, et al. , 2017. Deformability-based microfluidic separation of pancreatic islets from exocrine acinar tissue for transplant applications. Lab Chip 17 (21), 3682–3691. 10.1039/C7LC00890B. [PubMed: 28975176]

Wang DM, Tarbell JM, Aug. 1995. Modeling interstitial flow in an artery wall allows estimation of wall shear stress on smooth muscle cells. J. Biomech. Eng. 117 (3), 358–363. 10.1115/1.2794192. [PubMed: 8618390]

Xie R, Zheng W, Guan L, Ai Y, Liang Q, 2020. Engineering of hydrogel materials with perfusable microchannels for building vascularized tissues. Small 16 (15), 1902838. 10.1002/smll.201902838.

Yang CY, Cai SJ, Liu H, Pidgeon C, Jan. 1997. Immobilized Artificial Membranes — screens for drug membrane interactions. Adv. Drug Deliv. Rev. 23 (1), 229–256. 10.1016/S0169-409X(96)00438-3.

Zhang R, Larsen NB, 2017. Stereolithographic hydrogel printing of 3D culture chips with biofunctionalized complex 3D perfusion networks. Lab Chip 10.

Zheng Y, et al. , Jun. 2012. In vitro microvessels for the study of angiogenesis and thrombosis. Proc. Natl. Acad. Sci. Unit. States Am. 109 (24), 9342–9347. 10.1073/pnas.1201240109.

Zhu Y, et al. , 2020. Amnion-on-a-chip: modeling human amniotic development in mid-gestation from pluripotent stem cells. Lab Chip 20 (17), 3258–3268. 10.1039/D0LC00268B. [PubMed: 32749421]

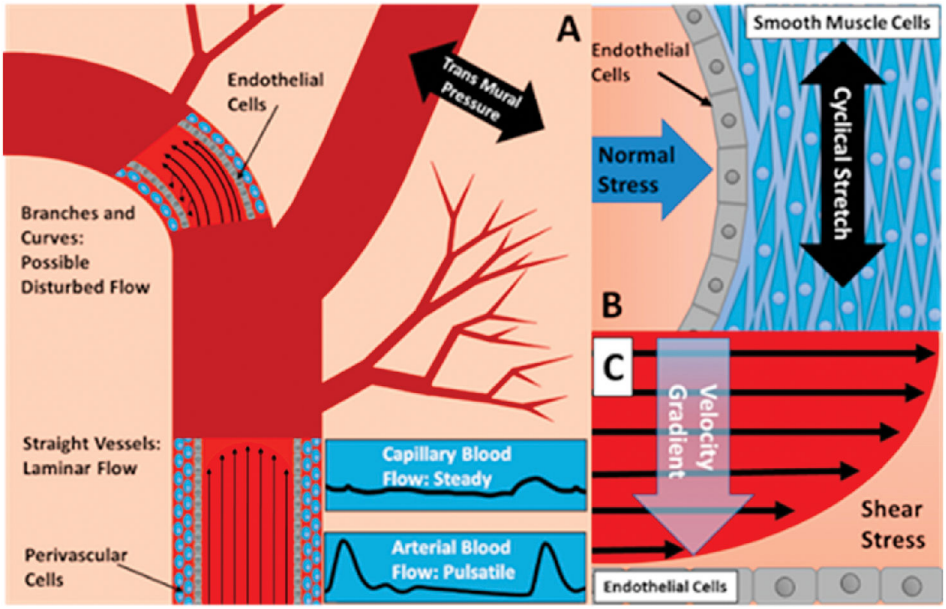

Fig. 1.

Effect of mechanical factors on: **A:** tissue around vasculature B: cyclical stretch C: shear stress incident on endothelial cells.

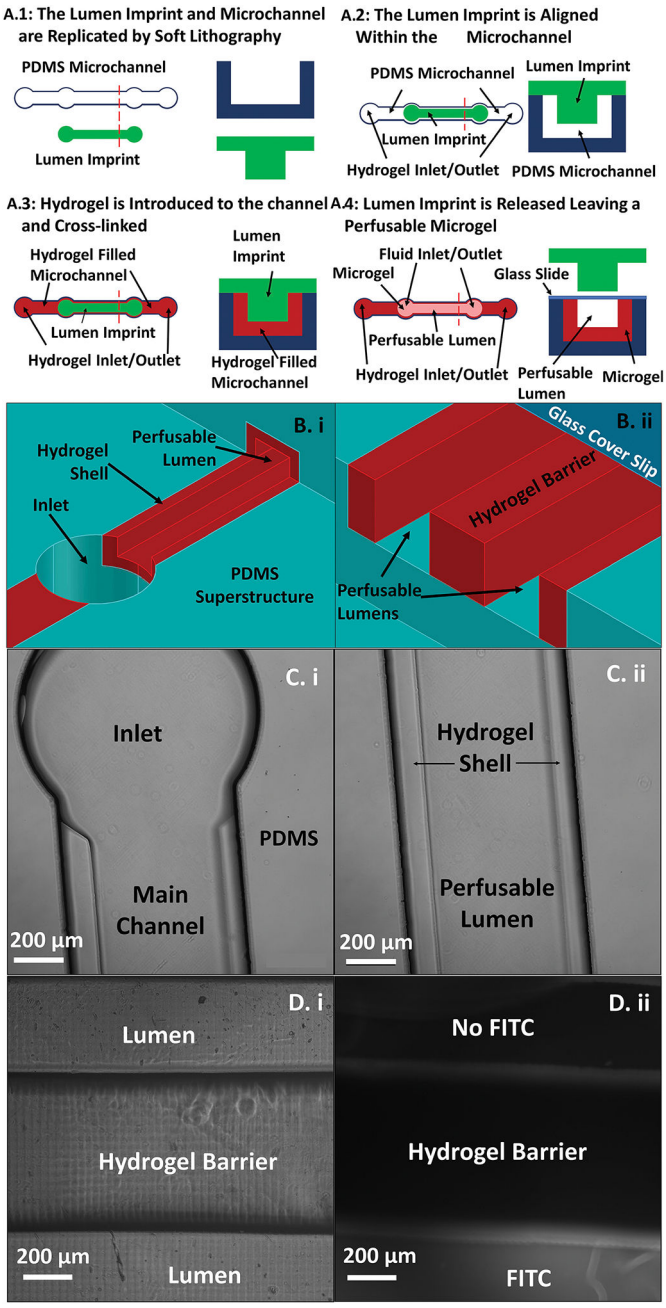

Fig. 2.

A: Process flow for fabrication of single lumen structures. **B.i-ii:** Cut away diagram of the single and double lumen co-culture device. **C.i-.ii**: Image of the fluidic inlet and main channel for the single lumen co-culture device. **D.i:** bright field Image of 500 µm hydrogel structure flanked by two 500 µm individually addressable lumens. **D.ii:** Florescent image of hydrogel barrier interceding lumens filled with unlabelled and FITC labelled Poly-L-Lysine using addressable fluid channels.

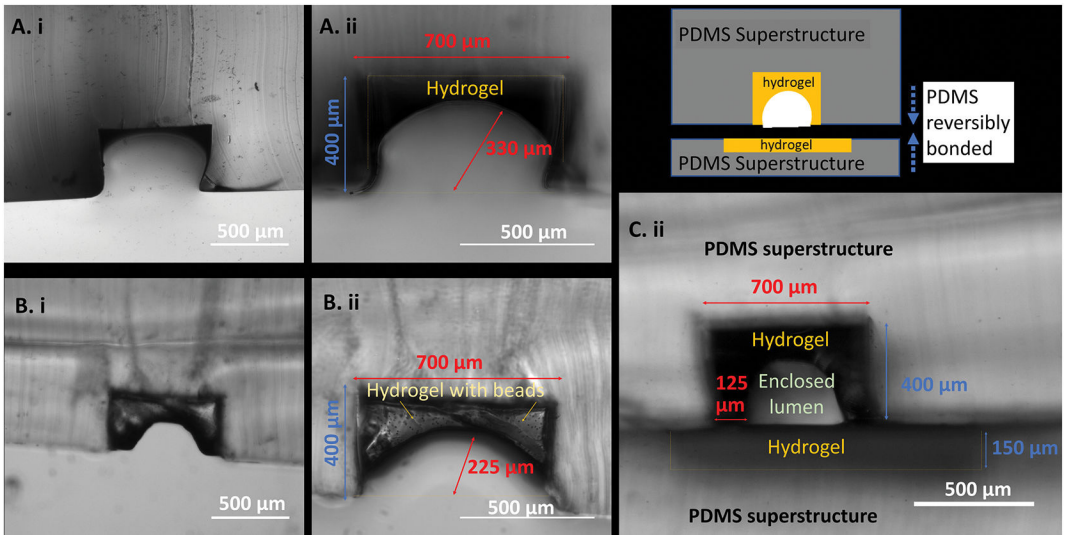

Fig. 3.

Circular hydrogel structures created to resemble vasculatures of varying cross-sectional diameters (A and B) imaged at different magnifications (i (4×) and ii (10×)) after sectioning the chip. The image (B) is shown with beads to mimic cell-laden hydrogels. Schematic for fabrication of lumen enclosed on all sides by hydrogel (C. i), as per image after sectioning (C. ii).

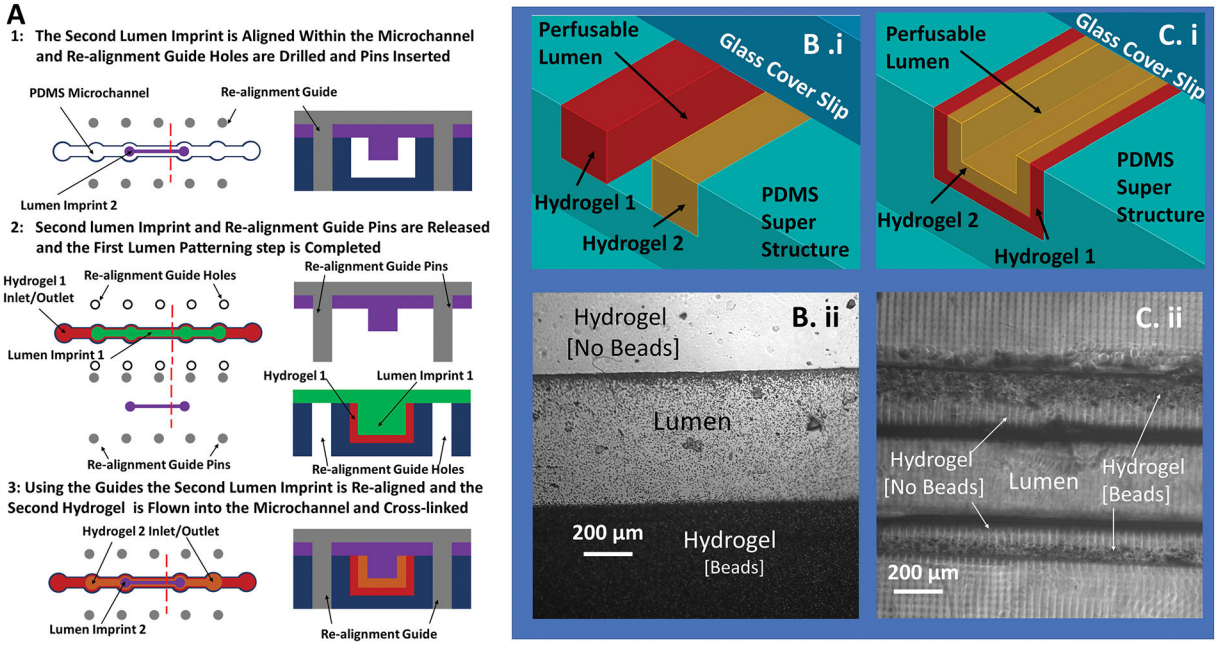

Fig. 4.

A. Process flow for fabricating devices requiring multiple imprints based on 3D printed constructs for alignment of hydrogels over multiple layers without desiccation. **B.i-.ii:** Schematic (i) and respective brightfield image (ii) of a multi-biomaterial structure with two individually patterned hydrogels separated by a lumen. Beads are added to the first hydrogel to improve image definition. **C.i-.ii:** Schematic (i) and respective brightfield image (ii) of a perfusable hydrogel with two individually patterned hydrogel shells around a single lumen. Beads added to the first hydrogel to demonstrate layer definition.

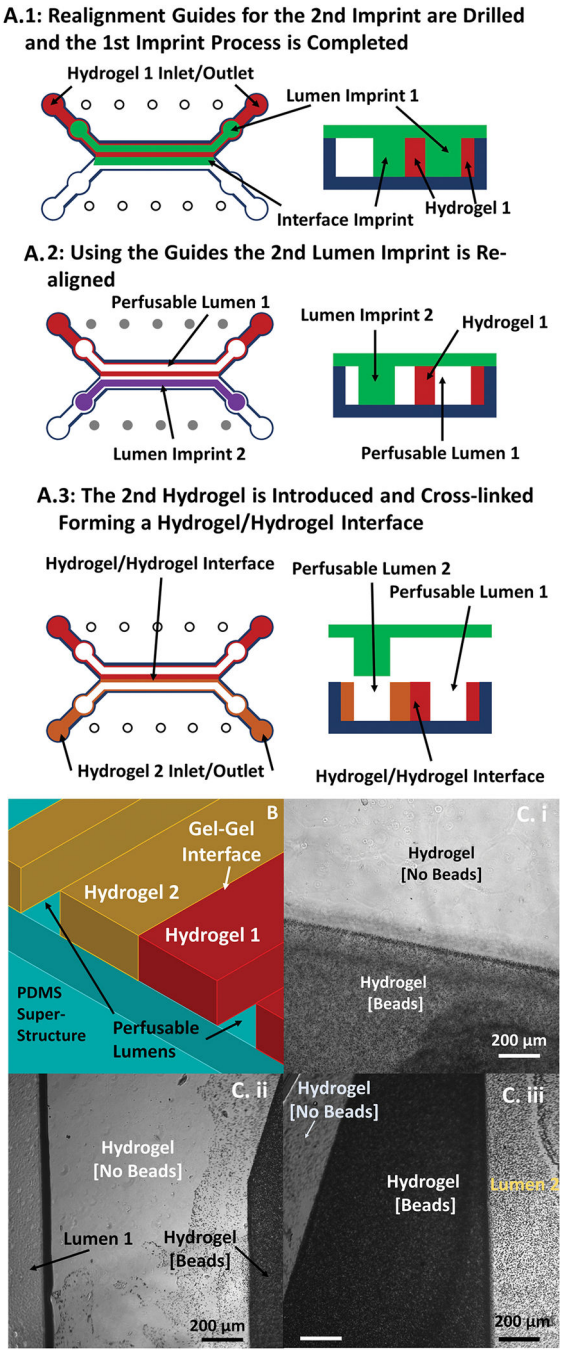

Fig. 5.

A. Process flow for patterning a microgel featuring interfaces between two biomaterials. **B:** Schematic 3D model of final device structure. **C i.-iii**: bright field images of different regions of a device with two individually patterned hydrogel structures. These structures are patterned to form a gel-gel interface between them, with ability to modulate length of the interface. The entire structure is flanked on either side by a perfusable 500 µm lumen. Beads are added to the initially patterned hydrogel structure for enhancing image definition.

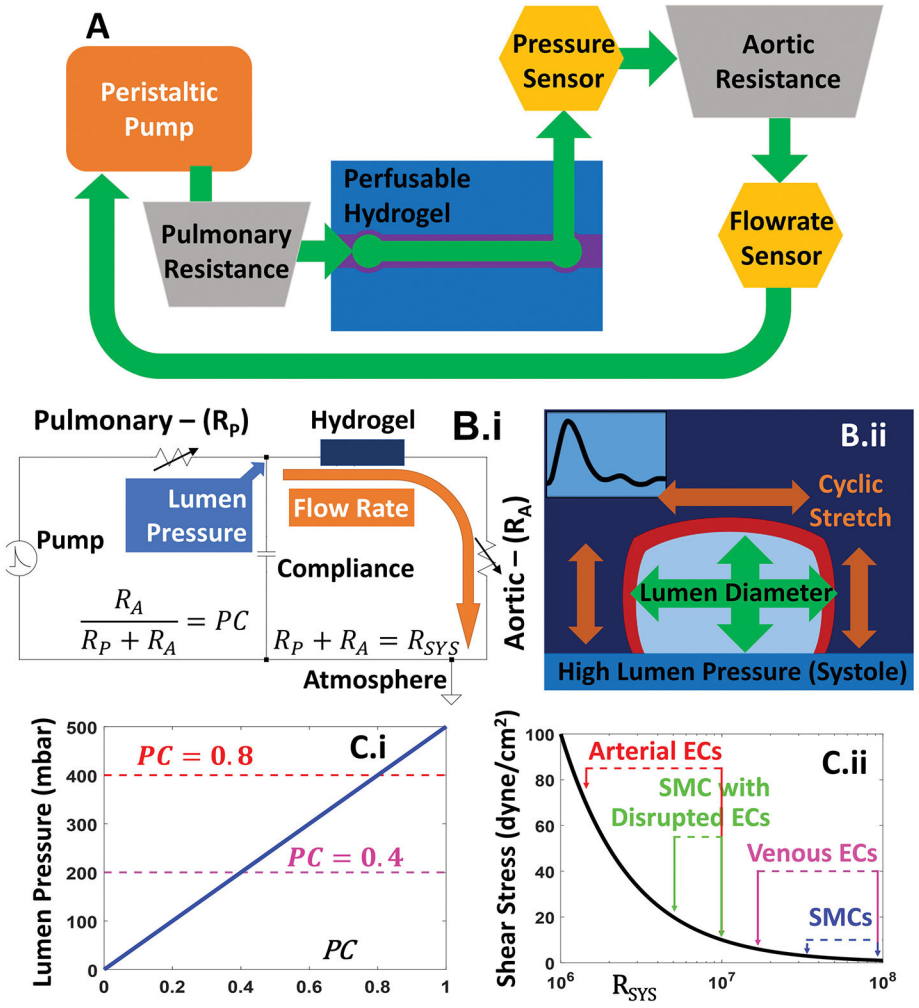

Fig. 6.

Schematic (**A**) and circuit model (**B.i**) of fluidics for perfusion of hydrogel channel. (**B.ii**) Increase in lumen pressure leads to diameter expansion causing cyclic stretch. The net system resistance (R_{SYS}) and pressure correction factor (PC), determined by pulmonary (R_P) and aortic (R_A) resistances elements, are tuned to independently set the lumen pressure (**C.i**) and flow rate in the channel, with the former regulating cyclic stretch and the latter regulating shear stress (**C.ii**), as shown for a range of cell models.

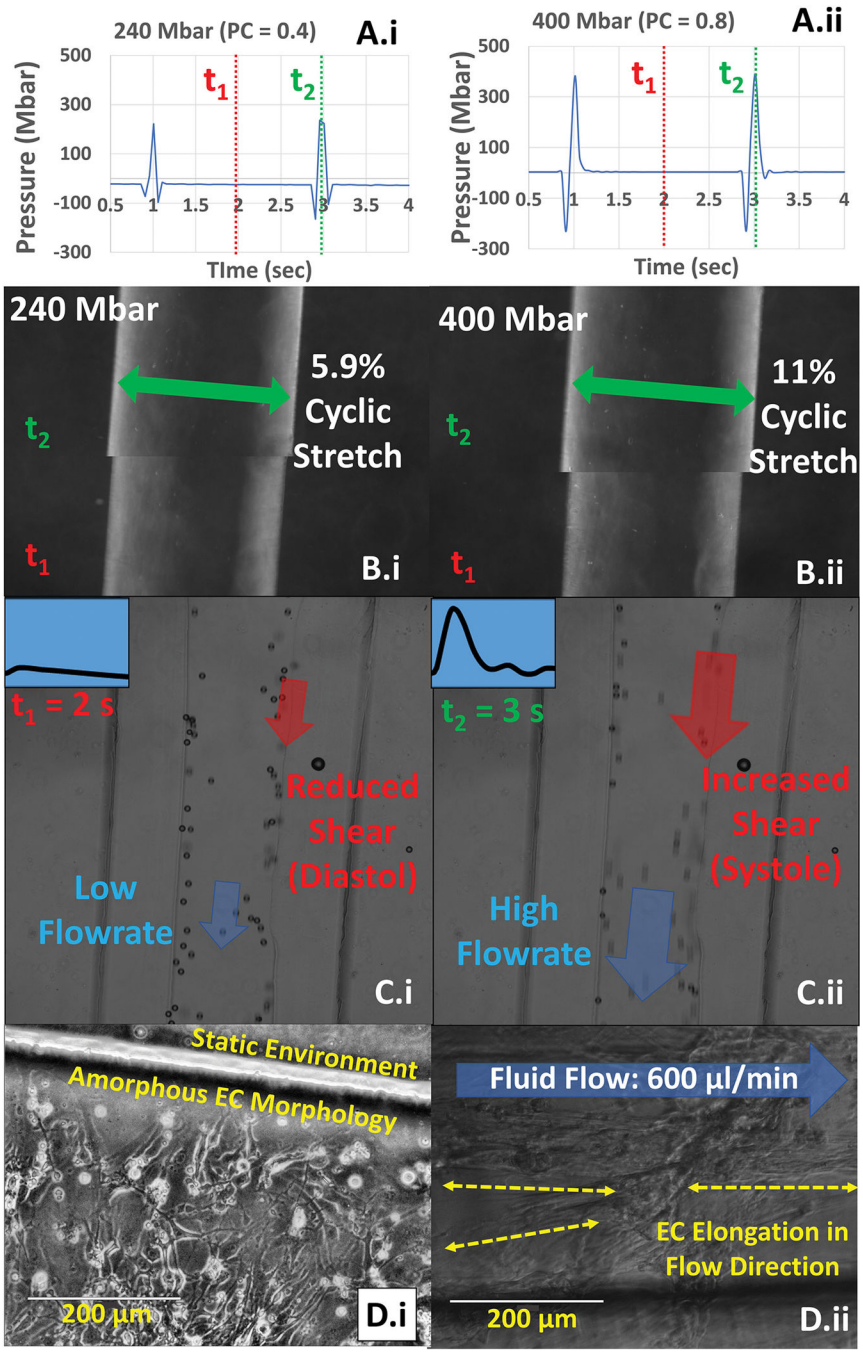

Fig. 7.

The effect of two different pressure pulses from initial state (t_1 = 2 s) to final state (t_2 = 3 s) of 240 mbar (A.i) and 400 Mbar (A.ii) cause cyclic stretch levels of 5.9% (B.i) and 11% (B.ii). Shear stress due to flow rate variations (C.i vs. C.ii) alter endothelial cell morphology to cause alignment along flow (D.i vs D.ii) (movie files: Shear.mp4 & CyclicStretch.mp4 in ESI†).

Table 1

Tuning resistor values (R_{sys}, R_A and R_P) to modulate cell model specific wall shear (Fig. 6C. ii) and the *PC* value that alters lumen pressure (Fig. 6C. i) to influence cyclical stretch (Note that $R_P = R_{SYS} - R_A$).

Cell Model	Wall Shear Stress (dynes/cm^2)	R_{SYS} (10^7 Pa s/cm^3)	R_a (PC = 0.8) (10^7 Pa s/cm^3)	R_a (PC = 0.4) (10^7 Pa s/cm^3)
SMCs	1.0–3.0	10.0–3.34	8.0–2.67	4.0–1.33
SMCs (Disrupted ECs)	10.0–20.0	1.01–0.5	0.804–0.4	0.402–0.2
ECs Venous	1.0–6.0	10.0–1.67	8.0–1.33	4.0–0.667
ECs Arterial	10.0–70.0	1.01–0.143	0.804–0.114	0.402–0.0572